

# Imaging Studies for Preoperative Planning of Perforator Flaps: An Overview



Shimpei Ono, MD, PhD<sup>a,\*</sup>, Hiromitsu Hayashi, MD, PhD<sup>b</sup>,  
Hiroyuki Ohi, MD<sup>c</sup>, Rei Ogawa, MD, PhD<sup>a</sup>

## KEYWORDS

• MDCT • Perforator flap • Propeller flap • CT angiography • Suprafascial perforator directionality

## KEY POINTS

- For safely planning perforator flaps, accurate preoperative assessment of perforators is recommended because their vascular anatomy varies between individuals.
- To assist in preoperative perforator assessment, perforator computed tomographic angiography (P-CTA) with multidetector-row computed tomography is currently one of the best available methods.
- The location of reliable perforators and their subcutaneous course between the deep fascia and skin, known as suprafascial perforator directionality, can be accurately determined preoperatively using P-CTA.
- Using P-CTA, surgeons can share 3-dimensional information of the perforator's location, diameter, and course, in relation to other anatomic structures preoperatively in a short time, which can shorten operative time and improve operative outcomes.

## INTRODUCTION

Perforator flaps have been gaining popularity over the last decade in the reconstructive surgery field. Advances in perforator-flaps transfer techniques allow harvesting of thin, pliable, and well-vascularized cutaneous flaps with minimal donor site morbidity as a consequence of the preservation of innervation, vascularization, and functionality of the underlying donor muscle. Perforator flaps are usually harvested as island flaps separated from all the surrounding skin and nourished by only one or 2 perforators arising from the deep major artery (**Fig. 1**). Vascular anatomy of perforators varies between individuals; therefore,

accurate preoperative determination of the location of reliable perforators and their subcutaneous course between the deep fascia and skin is important for safely planning perforator flaps.

To assist in preoperative perforator assessment, perforator computed tomographic angiography (P-CTA) with multidetector-row computed tomography (MDCT) has been developed to reveal the anatomic details of individual flap perforators.<sup>1</sup> MDCT differs from traditional computed tomography (CT) in that the scanner array has multiple detector rows in the scanning direction as opposed to just one detector row in traditional CT, allowing for acquisition of more than one image per

Funding Sources: None.

Conflict of Interest: None.

<sup>a</sup> Department of Plastic, Reconstructive, and Aesthetic Surgery, Nippon Medical School, 1-1-5 Sendagi, Bunkyo-ku, Tokyo 113-8603, Japan; <sup>b</sup> Department of Radiology, Nippon Medical School, 1-1-5 Sendagi, Bunkyo-ku, Tokyo 113-8603, Japan; <sup>c</sup> Hand & Microsurgery Center, Seirei Hamamatsu General Hospital, 2-12-12 Sumiyoshi, Naka-ku, Hamamatsu-shi, Shizuoka 430-0906, Japan

\* Corresponding author. Department of Plastic, Reconstructive, and Aesthetic Surgery, Nippon Medical School, 1-1-5 Sendagi, Bunkyo-ku, Tokyo 113-8603, Japan.

E-mail address: s-ono@nms.ac.jp

Clin Plastic Surg 44 (2017) 21–30

<http://dx.doi.org/10.1016/j.cps.2016.09.004>

0094-1298/17/© 2016 Elsevier Inc. All rights reserved.

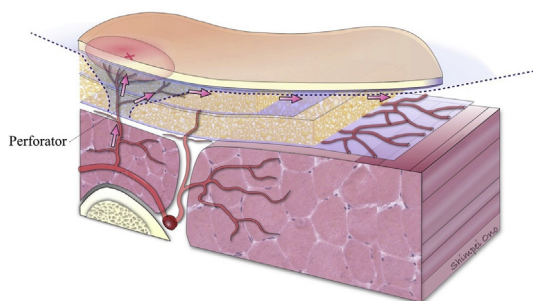


**Fig. 1.** The course of perforators. Red cross: the point where the perforator penetrates the deep fascia. Pink arrows: vascular flow from the perforator to the subdermal vascular network.

revolution of the x-ray detector tube around the patients. Thus, MDCT provides several thin-sliced CT images obtained in a short time. Compared with the product image provided by traditional single-detector-row CT, the higher number of thin-sliced CT images from MDCT provides increased spatial resolution in the resulting product image allowing for a multiplanar evaluation of perforators and 3-dimensional images of the perforating vessels.

The aim of this report is to describe the authors' experience using P-CTA with MDCT in detecting the perforators preoperatively and a step-by-step approach to harvest perforator flaps based on this technique.

## STEP-BY-STEP APPROACH TO HARVEST OF PERFORATOR FLAPS

### Case Presentation

A 37-year-old male truck driver presented with a pilonidal sinus in the sacrococcygeal region (**Fig. 2**). The patient had symptoms of the disease with multiple recurrent abscesses and spontaneous drainage for more than 5 years. A perforator-based propeller flap vascularized by the superior gluteal artery perforator (SGAP) was planned to cover the

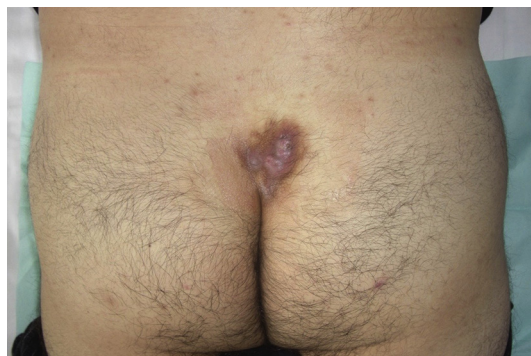


**Fig. 2.** A pilonidal sinus in the sacrococcygeal region.

defect after the pilonidal sinus resection. Perforator-based propeller flap, a type of pedicled perforator flaps, is an island flap in which flap movement is achieved by rotation around its vascular (perforator) axis (**Fig. 3**).<sup>2,3</sup> The perforator axis itself is stationary, and flap movement is achieved by rotation around this perforator. It has been so called because it is like a propeller in which the blades rotate around a fixed axis.<sup>2</sup>

### Perforator computed tomographic angiography

Because a perforator-based propeller flap is usually nourished by one or 2 perforators, preoperative assessment of candidate perforators is an important step in designing the flap. In this case, the SGAP was selected as the flap's pedicle. P-CTA analyses used 64-row MDCT (Light Speed VCT; GE Healthcare, Waukesha, WI) and were performed by a team including plastic surgeons, radiologists, and radiology technicians (**Fig. 4**). Scan parameters are summarized in **Table 1**.<sup>4</sup> The patient was scanned in a prone position similar to the operative positioning in which the normal contours of the buttock fat are not distorted by the pressure of lying against a flat surface. The scan range was limited by the superior border of the iliac bone to the gluteal fold to include tissues that will be used intraoperatively. The scan was performed with a rotation speed of 0.4 seconds per rotation, detectors coverage of 40 mm, and a detector configuration of 0.625 mm and 64 rows. This acquisition protocol allowed for a table speed of 137.5 mm/s and a scan time of less than 10 seconds for CTA.

For CTA, axial images of 0.625-mm thickness were reconstructed with an interval of 0.3 mm overlapping technique (eg, a 50% overlap means that half of the current image slab is covered by the preceding image and the other half by trailing image. Each point in the scanned volume is contained in exactly two reconstructed images. This would improve quality of MPR and volume images) and transferred to a workstation (Advantage Workstation; GE Healthcare, Chicago, IL) in the department of radiology or to a personal computer (Macintosh OSX; Apple Inc, Cupertino, CA) having an open-source digital imaging and communications in medicine (DICOM) image viewer software (OsiriX software; Pixmeo, Geneva, Switzerland) installed on it. The CTA images were reconstructed using maximum-intensity projection and volume-rendering techniques (**Fig. 5**).

### Selection of perforator

A couple of candidate perforators suitable to act as the pedicle of a flap were easily identified around the defects in the reconstructed images.

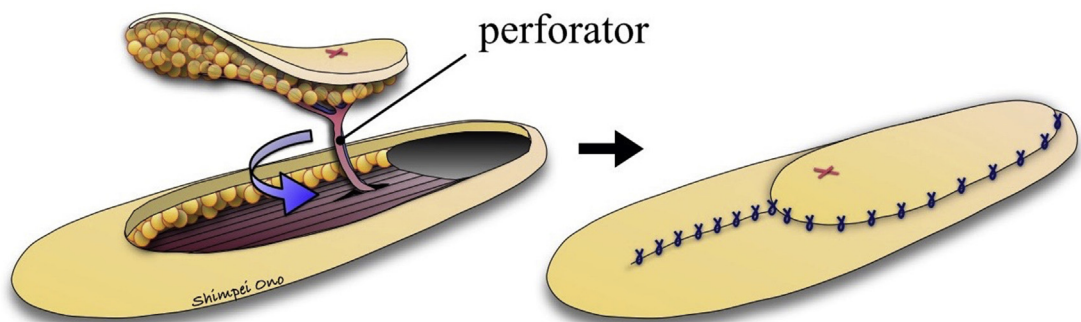


**Fig. 3.** A perforator-based propeller flap. Red cross: the point where the perforator penetrates the deep fascia.

Selection of a proper perforator is based on 2 criteria. The first is the perforator’s location. If 2 perforators of almost the same diameters can be found around the defect, the closer perforator to the defect is preferred because using the closer perforator minimizes the flap size, resulting in less vascular complications at the flap end. The second criterion is the perforator’s size. A measurement tool can measure the diameter of perforators. If 2 perforators are located at almost the same distances from a defect, the perforator with the larger diameter should be selected. A perforator greater than 1.0 mm in diameter is reliable for vascularity as a flap pedicle perforator.

**Assessment of 3-dimensional course of perforators**

The location where the selected perforator penetrates the deep fascia of the gluteus maximus muscle was indicated by a solid yellow circle in the image (Fig. 6). The distance from the circle to important anatomic landmarks, such as the midline or the prominence of the bone, can be measured, allowing the authors to draw marks on the patient’s skin and making the flap design easier. In addition, by using the multiplanar reconstruction view (Fig. 7), the course of the suprafascial perforator branches was traced on the

computer. This directionality between the deep fascia and skin is known as suprafascial perforator directionality (SPD), and including it in perforator-flaps’ design is considered a key indicator of

**Table 1**  
**Multidetector-row computed tomography scan parameters**

Parameter	
Scanner	64-slice MDCT scanner (LightSpeed VCT; GE Healthcare, Milwaukee, WI)
Detector configuration	64-row × 0.625-mm slice thickness
Detector coverage	40 mm
Helical detector pitch	0.516–0.984
Gantry rotation speed	0.4 s/rot
Tube potential	120 kVp
Tube current	600 mA (dose modulation)
Contrast	Iopamidol 370 mgI/mL (Iopamiron 370, Bayer Yakuhin Ltd, Osaka, Japan)
Volume	BW × (0.8–1.0) mL + Physiological saline 20 mL
Injection rate	BW × (0.08–0.1) mL/s (upper limit: 5 mL/s)
Bolus tracking method	SmartPrep
Initiation of CT scanning	Increase of >150 HU at aorta or the parent artery from which perforators emerge
Image reconstruction	0.3-mm overlapping axial images



**Fig. 4.** The CT room with a radiologist and radiology technician.

*Abbreviations:* BW, body weight; HU, Hounsfield units; mgI, mg iodine.

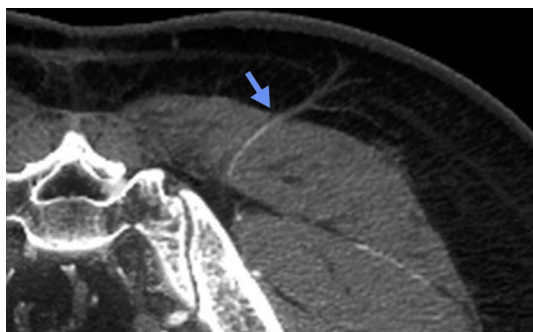


**Fig. 5.** Blue arrow shows the superior gluteal artery perforator.

reliable flap harvesting.<sup>5</sup> The authors' previous study revealed that many small branches diverge from the suprafascial perforator branch itself and reach the subdermal vascular network to nourish the overlying dermis (**Fig. 8**). SPD length was measured by using the software's measurement tool.

### **Flap design**

The detected point where a perforator penetrates the deep fascia on the computer was marked on the patient's skin. At that time, information about the distance from midline to the perforator was used, which was measured previously (**Fig. 9**). An SGAP-based propeller flap was designed including a perforator as flap pedicle and the SPD along the flap's long axis. The distance from the pedicle to the flap's distal end (A in **Fig. 10**) should be slightly longer, approximately 10% to 20%, than the length from the pedicle to the defect's distal edge (B in **Fig. 10**) to avoid closure with excessive tension on the flap's edges during suturing.

### **Flap elevation**

Flap elevation was performed under magnification loupes (2.5–4.0 ×) or microscopes with microsurgical instruments and technique. The initial incision



**Fig. 6.** The solid yellow circle indicates the point where the perforator penetrates the deep fascia of the gluteus maximus muscle.

was made along one lateral border of the flap. It is preferable to do a subfascial dissection initially because it is easier. With increasing experience, a suprafascial dissection will allow a thinner flap to be raised. One should be careful not to injure a suprafascial perforator branch detected preoperatively when thinning the flap. The flap was carefully raised until the previously marked perforator was visualized. The perforator identified by P-CTA preoperatively was located accurately intraoperatively without any errors (**Fig. 11**). Consequently, it was not required to change the flap design intraoperatively. After identifying the reliable perforator visually, an additional incision was made circumferentially to harvest the flap as an island flap.

### **Flap rotation and inset**

Before the flap is rotated into the defect, it is important to allow for flap perfusion and for the spasm in the vessels to relax for at least 10 to 15 minutes. The extent of dissection of the perforator depends on the degree of flap rotation required. The perforator is dissected to the point at which the flap can be rotated easily into the defect by carefully dividing any fibrous strands along the pedicle that impede this rotation. After rotating the flap, its pedicle should be checked for twisting or stretching. If any limitation exists, the pedicle should be further dissected into the muscle by keeping a sufficient pedicle length to relieve torsion on the pedicle, thereby allowing for adequate circulation. Preoperative P-CTA can help surgeons to safely dissect the pedicle into muscle. In the authors' case, the SGAP flap was rotated 135° clockwise without any vascular complications (**Fig. 12**). The donor defect after flap transfer was closed linearly, and a suction drain was securely placed well away from the pedicle.

## **DISCUSSION**

The choice of preoperative assessment tools in the planning of perforator flaps is still a controversial topic in reconstructive surgery. There are 4 main tools that can be used to assess perforators preoperatively: handheld acoustic Doppler sonography (ADS), color duplex sonography (CDS), P-CTA with MDCT, and magnetic resonance angiography (MRA). Characteristics of these 4 tools are summarized in **Table 2**.

### **Handheld Acoustic Doppler Sonography**

ADS is widely used because it is easy to operate, relatively inexpensive, portable, and available intraoperatively (**Fig. 13**). However, it has been reported that ADS is less accurate in identifying

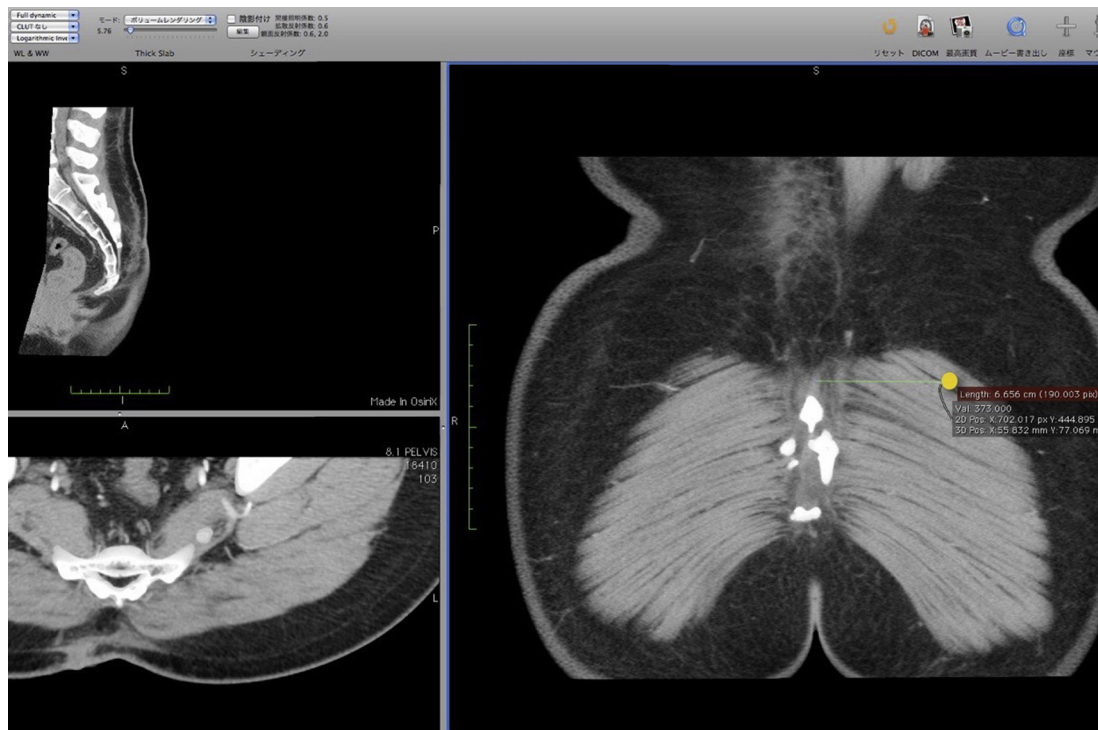


**Fig. 7.** The course of the suprafascial perforator branches can be traced by using multiplanar reconstruction view (*solid yellow circle* indicates the point where the perforator penetrates the deep fascia of the gluteus maximus muscle).

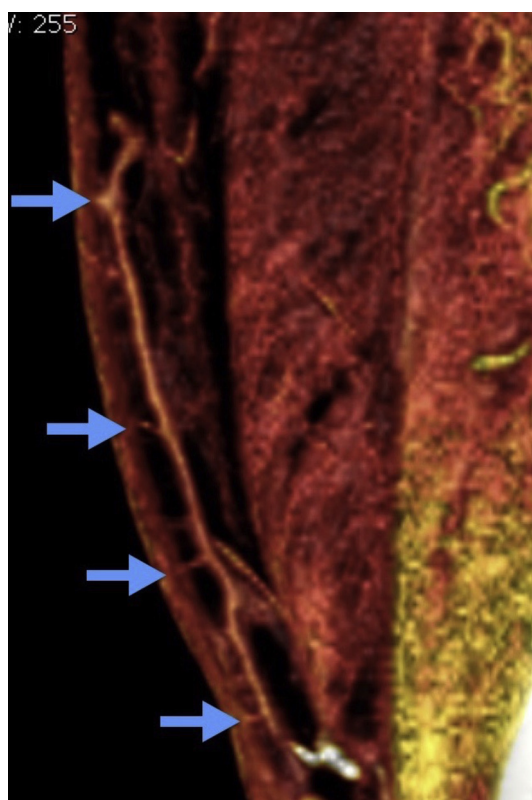


**Fig. 8.** Many small branches (*blue arrows*) diverged from a suprafascial perforator branch reaching to the subdermal vascular network.

perforators preoperatively compared with CDS<sup>6-8</sup> and P-CTA<sup>9-12</sup> because the Doppler probe (8 MHz) can only detect vessels located up to 20 mm from the skin surface. If the skin and subcutaneous tissue are thick, detecting the point where perforators penetrate the deep fascia is difficult.<sup>6</sup> Therefore, ADS tends to generate false positives; this is exaggerated in thin patients and reversed in obese patients.<sup>13</sup> Another reason is that ADS

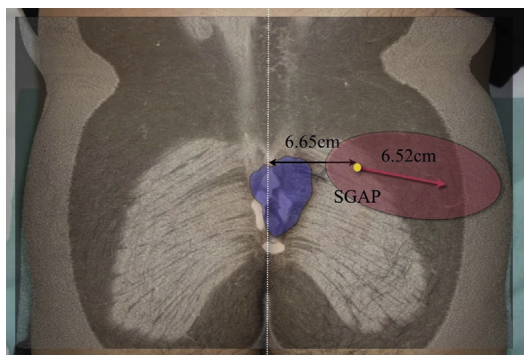


**Fig. 9.** An SGAP-based propeller flap (*red ellipse*) is designed including the perforator (*solid yellow circle*) as a pedicle and the SPD (*pink arrow*; its length is 6.52 cm). The blue area indicates the area affected by the pilonidal sinus. The distance from the midline to the perforator (*double-headed black arrow*) is 6.65 cm.

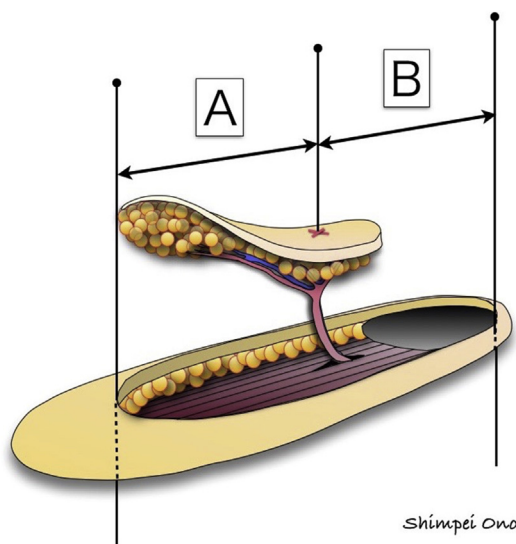


**Fig. 10.** Distance A (from perforator to the distal end of the flap) is slightly longer than distance B (from perforator to the distal edge of the defect). Red cross: the point where the perforator penetrates the deep fascia.



**Fig. 11.** Intraoperative photograph showing that the perforator identified preoperatively was located accurately during the operation without errors.



**Fig. 12.** Postoperative photograph. The flap was rotated 135° and the donor site was closed linearly.

cannot visualize vessels; thus, an examiner never knows for certain which vessels ADS detects. ADS may detect perforators that are too small to sustain a perforator flap; it is also too unspecific because of the background noise from vessels in the vicinity. ADS is recognized as less accurate in detecting perforators, but the authors prefer to use it in clinical practice. In addition to the advantages described earlier, ADS is useful as a screening for mapping perforators in free-style flaps' planning<sup>14</sup> and as a complementary tool to P-CTA or MRA. Furthermore, ADS can be available intraoperatively by using a sterilized probe or a probe cover to check the pulsation of a perforator during the operation.<sup>6</sup> When searching for perforators with ADS, signals that are pulsatile, loud, and high pitched can be consistently detected by the probe.<sup>15</sup> It has been suggested to vary the amount of pressure and angle applied with the probe to the skin surface. Prominent Doppler signal usually means the existence of a reliable perforator. With little experience, one can differentiate between Doppler signals from the main vessel versus those from perforators. The sound made by the main vessel will still be heard when the probe is moved proximally or distally, whereas the sound from a perforator is heard only at one location. Additionally, the sound from the main vessel is louder than that from the perforator.<sup>16</sup>

### Color Duplex Sonography

To overcome the disadvantages of ADS, CDS was developed as a noninvasive perforators' mapping device; it began to be used widely from the beginning of the 1990s.<sup>8,17–19</sup> The use of CDS spread rapidly because it provided more visual information about vessels compared with ADS. It could reveal not only the position of a perforator but also measure its diameter, course, and blood flow. The

**Table 2**  
**Characteristics of preoperative assessment tools in the planning of perforator flaps**

Preoperative Planning Tools	ADS	CDS	P-CTA	MRA
Portability	Excellent	Good	Not portable	Not portable
Cost/examination (\$)	None or low	Moderate (200)	Relatively high (400)	High (600)
Invasiveness	None	None	Injection of IV contrast	Injection of IV contrast
Operator dependence	Yes	Yes	No	No
Reproducibility	+	+	+++	++
Learning curve	Little	Significant	No	No
Accuracy of perforator detection	High false positive <sup>a</sup>	Relatively high	High	High
Hemodynamic information of perforator	No	Yes	No	No
Time to image acquisition	Depends on operator ( $\approx 10$ min)	Depends on operator ( $\approx 30$ min)	Short (<30 s)	Long (20 min)
Resolution (minimal detectable perforator caliber)	No image	0.5 mm	0.3–0.5 mm	1.0 mm
3D view	No image	No	Yes	Yes
Contrast material	—	—	+	+ (Safer risk profiles, eg, gadolinium)
Ionizing radiation exposure	—	—	+	—
Contraindications	None	None	Metal implants <sup>b</sup> Allergy to the contrast agent Renal insufficiency	

*Abbreviations:* 3D, 3 dimensional; IV, intravenous.

<sup>a</sup> A false positive rate is exaggerated in thin patients and reversed in obese patients.<sup>13</sup>

<sup>b</sup> Perforators may not be clearly determined because of the artifacts of metal implants.

major advantage of CDS compared with other assessment tools is its ability to provide hemodynamic information, such as flow velocity and pulsatility with time. However, there are several

disadvantages for this imaging tool. First, its uses are limited by the fact that it is relatively time consuming, taking approximately 30 minutes, and requires a skilled examiner who has knowledge of perforators' anatomy (see **Table 2**). Secondly, it is less reproducible because of its real-life dynamics<sup>20</sup> and does not allow for sharing of the 3-dimensional vascular images between surgeons. Thirdly, CDS can only provide the perforator's information in a limited area. CDS is very sensitive to the perforators in the superficial tissue layer, whereas it is less sensitive in deeper tissues because of the intermittent image capture. Furthermore, it does not provide the whole structural information about the perforator and adjacent anatomic landmarks in one image. Therefore, the authors recommend that the use of CDS should be limited to selected cases, such as patients with metal implants, allergy to the contrast agent, or renal insufficiency.

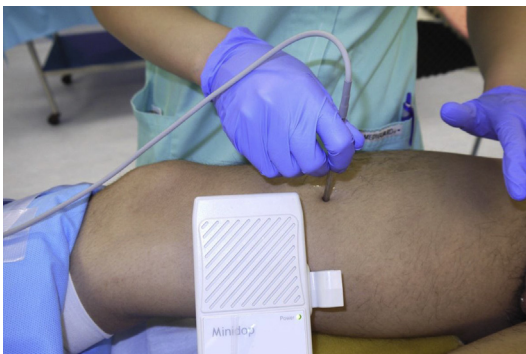


**Fig. 13.** Handheld ADS being done on the perforator site.

### Perforator Computed Tomographic Angiography

As described earlier, advancements in CT technology made it possible to reveal small perforators as narrow as 0.3 to 0.5 mm in diameter. Several investigators have reported the clinical usefulness of P-CTA with MDCT for preoperative detection of perforators.<sup>4,9,21–25</sup> P-CTA with MDCT can provide surgeons with detailed 3-dimensional images of vessels, including the perforator's location, diameter, and course, with its relation to other anatomic structures. Surgeons can share the images preoperatively in a short time, which can shorten operative time and improve operative outcomes.<sup>26</sup> Based on studies investigating abdominal perforators, P-CTA with MDCT enables the precise assessment of perforators, with a high sensitivity (96%–100%) and specificity (95%–100%).<sup>9,10,25</sup> In 3 studies comparing CDS with P-CTA, all the investigators<sup>23,27,28</sup> concluded that P-CTA was superior to CDS with regard to its accuracy in identifying perforators. The authors' past study, for assessing usefulness of preoperative P-CTA for 16 propeller flaps, revealed similar results.<sup>4</sup> All perforators identified by P-CTA preoperatively were accurately located during the operation without any errors. The distance between the estimated preoperative positions and the actual intraoperative positions were within 1 cm, and there were no false positives or negatives. Furthermore, in all cases but one, the operations finished on or before the scheduled time. On average, the actual operative time was 23% less than the scheduled time.

On the contrary, Feng and colleagues<sup>28</sup> reported that CDS is more accurate than P-CTA in the preoperative mapping of perforators in the lower extremity. This finding is based on 2 anatomic characteristics of the lower extremity: the relatively thin subcutaneous tissue and its tubelike 3-dimensional structure. Because P-CTA can provide a clearer perforator image based on sharp distinction between the density of the contrasted perforator (white) and fat tissue (black) in areas with less fat tissue, such as the lower extremity, it is not accurate enough in areas rich in fat tissue, such as the abdomen. They also mentioned that the rotation of the lower extremity could cause displacement of the skin surface from the deep tissue, leading to more errors in locating perforators by P-CTA. The authors agree that detection of perforators by P-CTA requires more careful observation of images in patients and anatomic sites with less fat tissue; however, P-CTA can provide detailed information about the perforator course in the deeper tissue layers

and the surrounding anatomic landmarks (Fig. 14). Furthermore, by taking P-CTA exactly on the same as the position in the operating room, we can minimize the displacement of detected perforators during operations.

Major disadvantages of P-CTA are the exposure to ionizing radiation and the use of potentially nephrotoxic contrast agent.<sup>9</sup> Moreover, metal components, such as an internal fixation plate or external fixator around target perforators, compromise the accuracy of their detection secondary to artifacts.

### Magnetic Resonance Angiography

Contrast-enhanced MRA has been developed recently for identifying the 3-dimensional anatomy of perforators with an accuracy approaching that of P-CTA. MRA is advantageous over P-CTA as it works with magnetism instead of radiation and can be performed with a noniodinated contrast medium, making it a safer examination for patients. Implanted metal devices or pacemakers are contraindications for MRA. Rozen and colleagues<sup>29,30</sup> reported in their 2 studies comparing

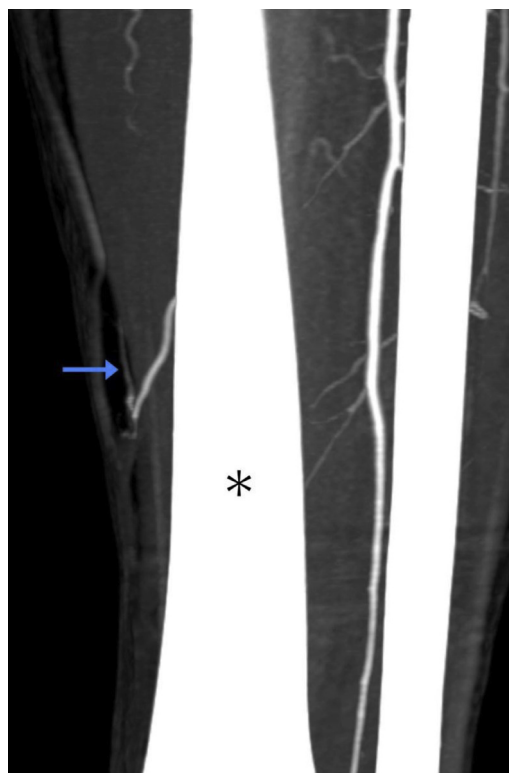


**Fig. 14.** Detailed information about the perforator course even in sites with less fat tissue (lower leg). Blue arrow: the posterior tibial artery perforator. Tibia (asterisk).

MRA with P-CTA that the depiction of smaller perforators, less than 1.0 mm, was less accurate with MRA. In conclusion, P-CTA is currently superior to MRA regarding accuracy in detecting smaller perforators; nevertheless, MRA has a future potential to become as accurate as CTA because it does not require radiation or iodinated contrast medium.

## SUMMARY

A comprehensive literature review shows that P-CTA with MDCT is highly accurate in identifying and mapping perforators preoperatively, although it uses radiation and contrast medium. Three-dimensional images of perforators and their surrounding anatomy allow easy interpretation by surgeons and can shorten the operative time improving the operative outcomes. Further studies are required to properly assess the role of P-CTA regarding costs and impact on patient outcomes.

## REFERENCES

1. Ono S, Ogawa R, Hayashi H, et al. Multidetector-row computed tomography (MDCT) analysis of the supra-fascial perforator directionality (SPD) of the occipital artery perforator (OAP). *J Plast Reconstr Aesthet Surg* 2010;63:1602–7.
2. Hyakusoku H, Yamamoto T, Fumiiri M. The propeller flap method. *Br J Plast Surg* 1991;44:53–4.
3. Teo TC. The propeller flap concept. *Clin Plast Surg* 2010;37:615–26.
4. Ono S, Chung KC, Hayashi H, et al. Application of multidetector-row computed tomography in propeller flap planning. *Plast Reconstr Surg* 2011;127:703–11.
5. Ono S, Ogawa R, Hayashi H, et al. How large a pedicled perforator flap can be harvested? *Plast Reconstr Surg* 2012;130:195e–6e.
6. Yu P, Youssef A. Efficacy of the handheld Doppler in preoperative identification of the cutaneous perforators in the anterolateral thigh flap. *Plast Reconstr Surg* 2006;118:928–35.
7. Khan UD, Miller JG. Reliability of handheld Doppler in planning local perforator-based flaps for extremities. *Aesthetic Plast Surg* 2007;31:521–5.
8. Tsukino A, Kurachi K, Inamiya T, et al. Preoperative color Doppler assessment in planning of anterolateral thigh flaps. *Plast Reconstr Surg* 2004;113:241–6.
9. Masia J, Clavero JA, Larrañaga JR, et al. Multidetector-row computed tomography in the planning of abdominal perforator flaps. *J Plast Reconstr Aesthet Surg* 2006;59:594–9.
10. Alonso-Burgos A, García-Tutor E, Bastarrika G, et al. Preoperative planning of deep inferior epigastric artery perforator flap reconstruction with multislice-CT angiography: imaging findings and initial experience. *J Plast Reconstr Aesthet Surg* 2006;59:585–93.
11. Puri V, Mahendru S, Rana R. Posterior interosseous artery flap, fasciosubcutaneous pedicle technique: a study of 25 cases. *J Plast Reconstr Aesthet Surg* 2007;60:1331–7.
12. Rozen WM, Phillips TJ, Ashton MW, et al. Preoperative imaging for DIEA perforator flaps: a comparative study of computed tomographic angiography and Doppler ultrasound. *Plast Reconstr Surg* 2008;121:9–16.
13. Shaw RJ, Batstone MD, Blackburn TK, et al. Preoperative Doppler assessment of perforator anatomy in the anterolateral thigh flap. *Br J Oral Maxillofac Surg* 2010;48:419–22.
14. Chang CC, Wong CH, Wei FC. Free-style free flap. *Injury* 2008;39:S57–61.
15. Wallace CG, Kao HK, Jeng SF, et al. Free-style flaps: a further step forward for perforator flap surgery. *Plast Reconstr Surg* 2009;124:e419–26.
16. Ono S, Sebastin SJ, Yazaki N, et al. Clinical applications of perforator based propeller flaps in upper limb soft tissue reconstruction. *J Hand Surg Am* 2011;36:853–63.
17. Rand RP, Cramer MM, Strandness DE Jr. Color-flow duplex scanning in the preoperative assessment of TRAM flap perforators: a report of 32 consecutive patients. *Plast Reconstr Surg* 1994;93:453–9.
18. Chang BW, Luethke R, Berg WA, et al. Two-dimensional color Doppler imaging for precision preoperative mapping and size determination of TRAM flap perforators. *Plast Reconstr Surg* 1994;93:197–200.
19. Hallock GG. Evaluation of fasciocutaneous perforators using color duplex imaging. *Plast Reconstr Surg* 1994;94:644–51.
20. Smit JM, Dimopoulou A, Liss AG, et al. Preoperative CT angiography reduces surgery time in perforator flap reconstruction. *J Plast Reconstr Aesthet Surg* 2009;62:1112–7.
21. Masia J, Larranaga J, Clavero JA, et al. The value of the multidetector row computed tomography for the preoperative planning of deep inferior epigastric artery perforator flap: our experience in 162 cases. *Ann Plast Surg* 2008;60:29–36.
22. Rozen WM, Ashton MW, Stella DL, et al. The accuracy of computed tomographic angiography for mapping the perforators of the deep inferior epigastric artery: a blinded, prospective cohort study. *Plast Reconstr Surg* 2008;122:1003–9.
23. Badiul PO, Sliesarenko SV. Multidetector-row computed tomographic angiography in the planning of the local perforator flaps. *Plast Reconstr Surg Glob Open* 2015;22:e516.
24. Yang SF, Wang CM, Ono S, et al. The value of multidetector row computed tomography angiography for preoperative planning of freestyle pedicled perforator flaps. *Ann Plast Surg* 2016. [Epub ahead of print].

25. Rosson GD, Williams CG, Fishman EK, et al. 3D CT angiography of abdominal wall vascular perforators to plan DIEAP flaps. *Microsurgery* 2007;27:641–6.
26. Uppal RS, Casaer B, Van Landuyt K, et al. The efficacy of preoperative mapping of perforators in reducing operative times and complications in perforator flap breast reconstruction. *J Plast Reconstr Aesthet Surg* 2009;62:859–64.
27. Imai R, Matsumura H, Tanaka K, et al. Comparison of Doppler sonography and multidetector-row computed tomography in the imaging findings of the deep inferior epigastric perforator artery. *Ann Plast Surg* 2008;61:94–8.
28. Feng S, Min P, Grassetti L, et al. A prospective head-to-head comparison of color Doppler ultrasound and computed tomographic angiography in the preoperative planning of lower extremity perforator flaps. *Plast Reconstr Surg* 2016;137:335–47.
29. Rozen WM, Stella DL, Bowden J, et al. Advances in the pre-operative planning of deep inferior epigastric artery perforator flaps: magnetic resonance angiography. *Microsurgery* 2009;29:119–23.
30. Rozen WM, Ashton MW, Stella DL, et al. Magnetic resonance angiography and computed tomographic angiography for free fibular flap transfer. *J Reconstr Microsurg* 2008;24:457–8.